

1 **Experimental study of liquid to air membrane energy exchanger**
2 **(LAMEE) performance by measuring its temperature fields**

3 Junze Chu, Ziwei Chen, Hongyu Bai, Jie Zhu*

4 Department of Architecture and Built Environment, the University of Nottingham

5 University Park, Nottingham, NG7 2RD, UK

6 *Corresponding author, E-mail address: jie.zhu@nottingham.ac.uk

7
8 **Abstract**

9 Many studies have already been conducted to assess liquid to air membrane energy exchanger
10 (LAMEE) performance by numerical and experimental methods. However, the LAMEE
11 temperature field is still an unknown area due to the operation difficult. In this study, an
12 experimental method is adopted to investigate the performance of LAMEE by measuring its
13 temperature fields. The effects of main parameters such as the solution temperature, solution
14 concentration and air relative humidity, are investigated. The results show that the air relative
15 humidity and solution temperature have negative influences on the LAMEE efficiency. It is
16 found that the total effectiveness reduces 2.7% and 7.7% when the air relative humidity
17 increases from 62% to 74%, and the solution temperature changes from 18°C to 26°C,
18 respectively. Increasing the solution concentration decreases the sensible effectiveness while
19 enhancing the latent and total effectiveness. The total effectiveness increases 3.5% as the
20 solution concentration increase from 30% by 39%. These results are useful to optimize the
21 LAMEE in the future.

22 **Key words:** Experimental method; parameter effects; LAMEE performance, temperature field.

23 **1. Introduction**

24 Energy crisis becomes a serious problem in recent years and buildings consume about forty
25 percent of the total energy [1]. Heating, cooling and ventilation take large proportion in the
26 building energy consumption, and people spend most of their time on indoor activities [2].
27 Liquid desiccant air conditioning (LDAC) system saves large amount of energy compared with
28 the traditional mechanical type in dealing with latent heat; low regeneration temperature means
29 that LDAC system can be powered by low grade thermal energy such as waste heat or

30 renewable energy, which shows the potential of its application in the rural areas and developing
 31 countries [3]. Carryover problem of LDAC can be avoided by applying semi-permeable
 32 membranes in dehumidifier and regenerator [4]. The semi-permeable membranes separate the
 33 air stream and desiccant solution to prevent the carryover of liquid desiccant droplets. In a
 34 liquid to air membrane energy exchanger (LAMEE), only water vapour and heat can pass
 35 through the membrane, while the solution is not allowed to go through the membrane. Although
 36 the membrane increases the moisture and heat transfer resistances in the LDAC, it provides a
 37 safety environment for human beings. There are a lot of numerical study for the LAMEE
 38 temperature field [5-10], however the experimental test of the temperature field is still not
 39 carried out. In this paper an experimental method is adopted to investigate the performance of
 40 a LAMEE by measuring its temperature fields. The experimental results of the LAMEE
 41 temperature fields can be applied for validating the numerical modelling; moreover, it could
 42 be used as the reference data for optimization of the LAMEE, for example, adjusting the
 43 solution distribution according to the temperature field (more solution at high temperature area).

44

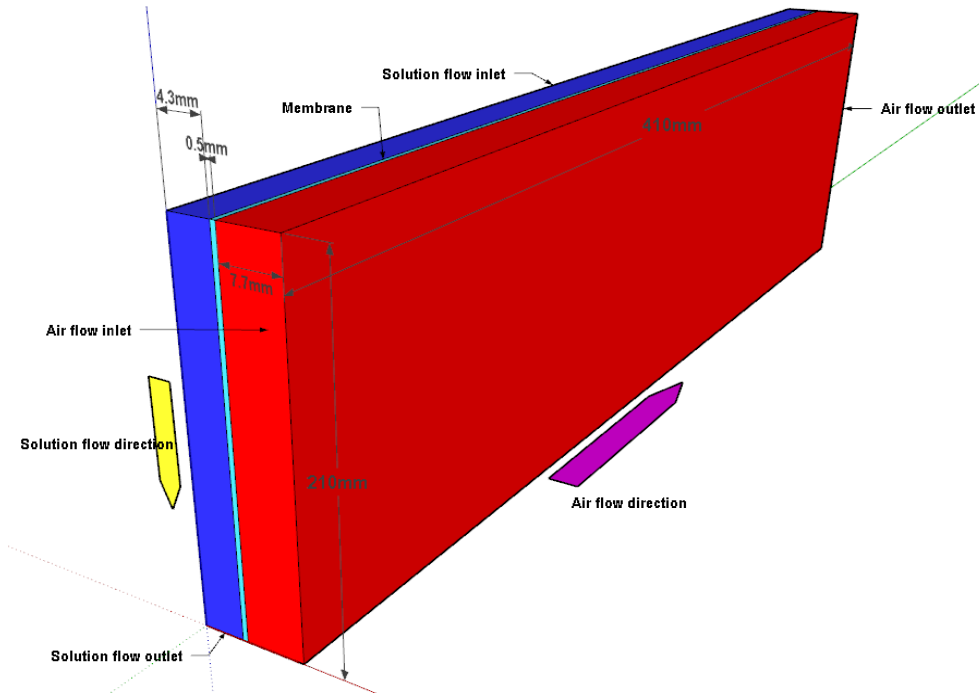
Nomenclature	
C	Concentration (kg/m^3)
c_p	Specific heat capacity (J/kgK)
Cr^*	Heat capacity ratio
d	Width of the channel (m)
D	Diffusivity (m^2/s)
H	Height of the LAMEE (m)
H^*	Operating factor
k	Thermal conductivity (W/mK)
k_m	Membrane water vapour permeability ($\text{kg}/\text{m s}$)
L	Length of the LAMEE (m)
LAMEE	Liquid to air membrane energy exchanger

LDAC	Liquid desiccant air conditioning
RH	Relative humidity (%)
T	Temperature (°C)
W	Width of the LAMEE (m)
$W_{air/sol}$	Humidity ratio (kg/kg)
Greek symbols	
ε	Effectiveness
δ	Membrane thickness (m)
ρ	Density (kg/m^3)
Subscripts	
air	Air flow
in	Inlet
lat	Latent
mem	Membrane
out	Outlet
sen	Sensible
sol	Solution flow
tot	Total

45

46 **2. Methodology**

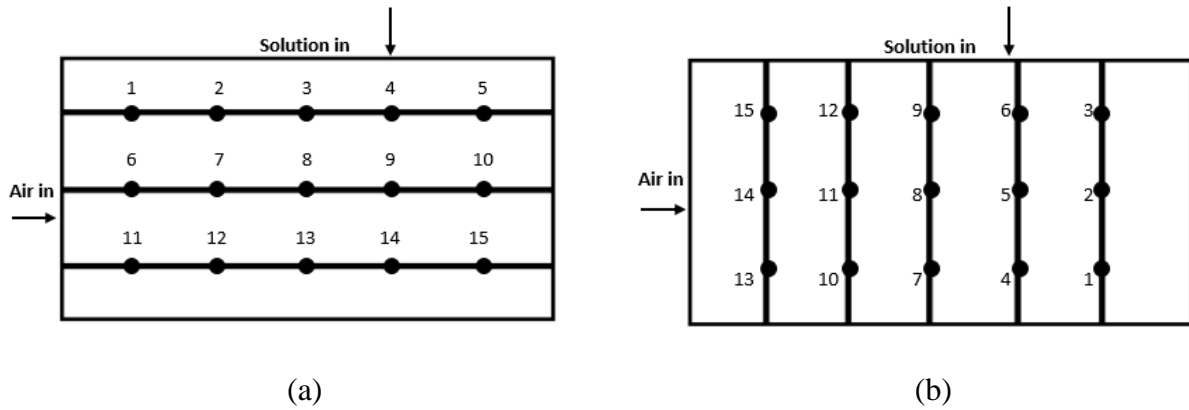
47 In order to get the temperature field inside the membrane based flat plate dehumidifier, a
48 number of temperature sensors are installed in one air channel and one adjacent solution
49 channel, the dehumidifier structure and geometry information are shown in Fig.1. Each channel
50 is installed with 15 sensors as indicated in Fig.2. In the air channel, every 5 sensors are stuck
51 in one strip in horizontal direction, while in the solution channel, every 3 sensors are fixed in
52 one strip in vertical direction.



54

55

Fig.1: Structure and geometry information for the air and solution channels.



56

57

Fig.2: Sensor arrangements in (a) air channel; (b) solution channel.

59 The specifications of the dehumidifier and membrane, and the desiccant solution and air
60 properties are listed in Table1.

61 Table 1: Dehumidifier specifications, membrane physical properties, air and desiccant solution
62 properties.

Symbol	Unit	Value	Symbol	Unit	Value
L	m	0.41	k_{air}	W/mK	0.03
W	m	0.23	k_{sol}	W/mK	0.53
H	m	0.21	D_{air}	m^2/s	2.46×10^{-5}

d_{air}	m	0.0077	D_{sol}	m^2/s	0.892×10^{-2}
d_{sol}	m	0.0043	$c_{p,air}$	J/kgK	1020
δ_{mem}	m	0.5×10^{-3}	$c_{p,sol}$	J/kgK	3200
k_{mem}	W/mK	0.3	ρ_{air}	kg/m^3	1.29
$k_{m,mem}$	Kg/ms	3.87×10^{-6}	ρ_{sol}	kg/m^3	1247

63

64 3. Performance index

65 Effectiveness is the commonly used performance index in energy exchanger. Sensible, latent
66 and total effectiveness are applied to investigate the energy exchanger performance
67 respectively. The sensible effectiveness is the ratio between the actual and maximum possible
68 sensible heat transfer rates in the energy exchanger and given by:

$$69 \quad \varepsilon_{sen} = \frac{T_{air,in} - T_{air,out}}{T_{air,in} - T_{sol,in}} \quad (1)$$

70

71 Where ε_{sen} is the sensible effectiveness, $T_{air,in}$ is the inlet air temperature ($^{\circ}C$), $T_{air,out}$ is the
72 outlet air temperature ($^{\circ}C$), $T_{sol,in}$ is the inlet solution temperature ($^{\circ}C$).

73 The latent effectiveness is the ratio between actual and maximum possible latent heat transfer
74 rates in the energy exchanger and defined as:

$$75 \quad \varepsilon_{lat} = \frac{W_{air,in} - W_{air,out}}{W_{air,in} - W_{sol,in}} \quad (2)$$

76

77 Where ε_{lat} is the latent effectiveness, $w_{air,in}$ is the inlet air humidity ratio (kg/kg), $w_{air,out}$ is
78 the outlet air humidity ratio (kg/kg), $w_{sol,in}$ is the inlet solution equilibrium specific humidity
79 ratio (kg/kg).

80

81 The total effectiveness is the ratio between the actual and maximum possible energy transfer
82 rates in the energy exchanger and given by:

$$83 \quad \varepsilon_{tot} = \frac{\varepsilon_{sen} + H^* \varepsilon_{lat}}{1 + H^*} \quad (3)$$

84

85 Where ε_{tot} is the total effectiveness, H^* is the operating factor.

86 Equations (1) to (3) are only meaningful when the solution capacity rate is higher than or equal
87 to the air capacity rate ($Cr^* \geq 1$).

88 4. Experiment setting

89 The basic experimental parameters are set as: 20°C inlet lithium chloride solution with 33%
 90 concentration; 30°C inlet air temperature with 70% relative humidity. The more detail settings
 91 are shown in Table 2.

92 Table 2 : Experiment settings.

Num	Air RH (%)	Num	T sol (°C) C _{sol} =30%	Num	T sol (°C) C _{sol} =33%	Num	T sol (°C) C _{sol} =36%	Num	T sol (°C) C _{sol} =39%
1	62	5	18	10	18	15	18	20	18
2	66	6	20	11	20	16	20	21	20
3	70	7	22	12	22	17	22	22	22
4	74	8	24	13	24	18	24	23	24
		9	26	14	26	19	26	24	26

93

94 30%, 33%, 36% and 39% concentration solutions are tested under five different inlet solution
 95 temperatures.

96

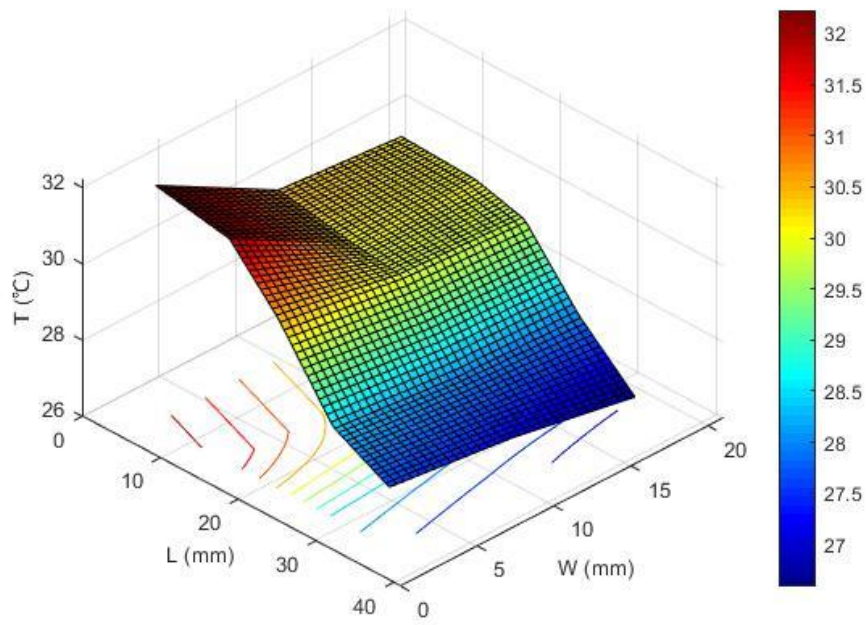
97 5. Results & discussion

98 The temperature field results for basic parameter setting are shown in Table 3. From Table 3,
 99 it can be seen that the air temperature decreases along its flow direction and increases in the
 100 vertical direction. As for the solution temperature, it increases along the solution flow direction,
 101 the highest temperature occurs at the left bottom corner. The temperature maps are plotted with
 102 linear interpolation method as shown in Fig.3.

103 Table 3: Temperature field results for basic parameter setting.

Air side (°C)					Solution side (°C)				
1	2	3	4	5	15	12	9	6	3
30.146	30.053	29.696	27.939	26.531	19.515	19.822	19.52	19.975	19.157
6	7	8	9	10	14	11	8	5	2
30.428	30.069	29.901	28.061	27.161	21.229	19.954	19.783	19.975	19.179
11	12	13	14	15	13	10	7	4	1
32.232	31.863	30.445	28.384	27.553	23.937	22.608	20.33	20.155	19.415

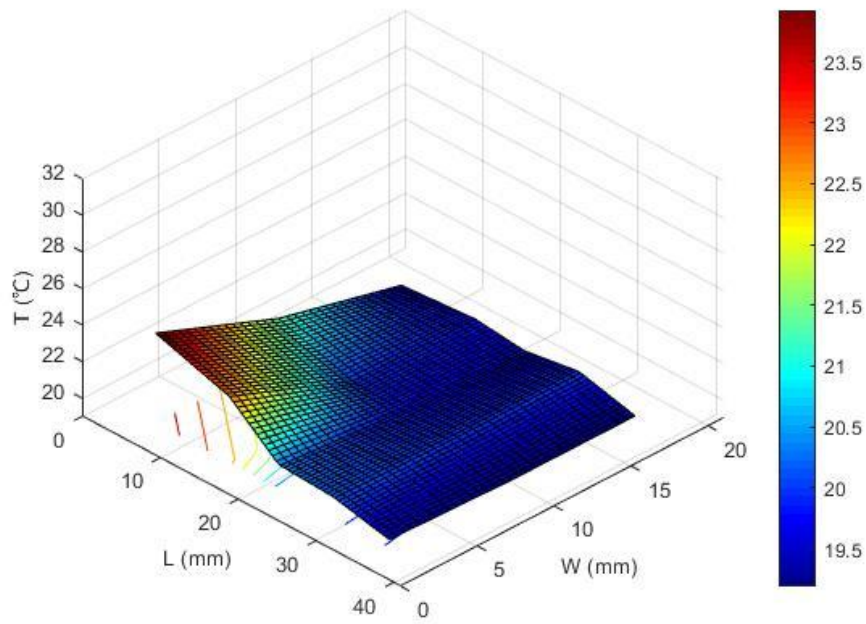
104



105

106

(a)



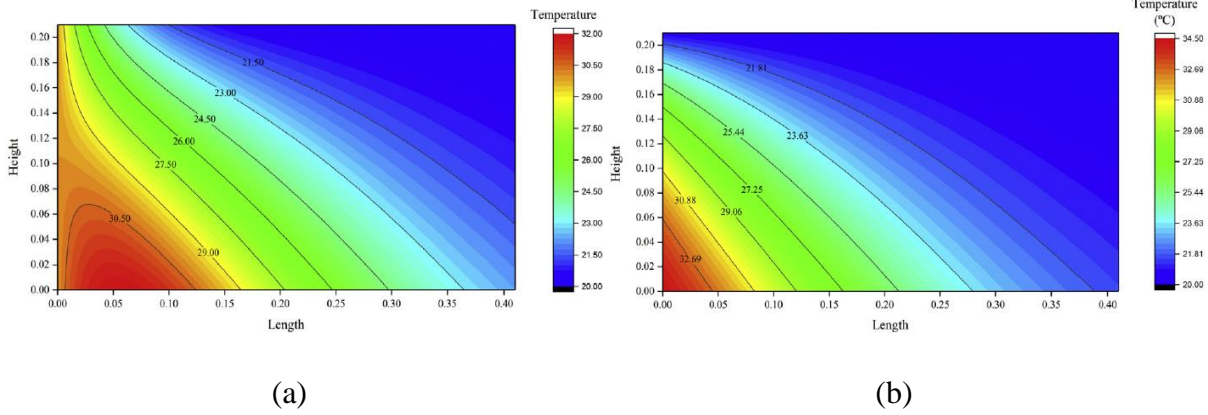
107

108

(b)

109

Fig.3: (a) Air temperature field; (b) Solution temperature field.



110

111

112

Fig.4: Temperature fields in previous work: (a) air side; (b) solution side [11].

113

114

115

116

117

118

119

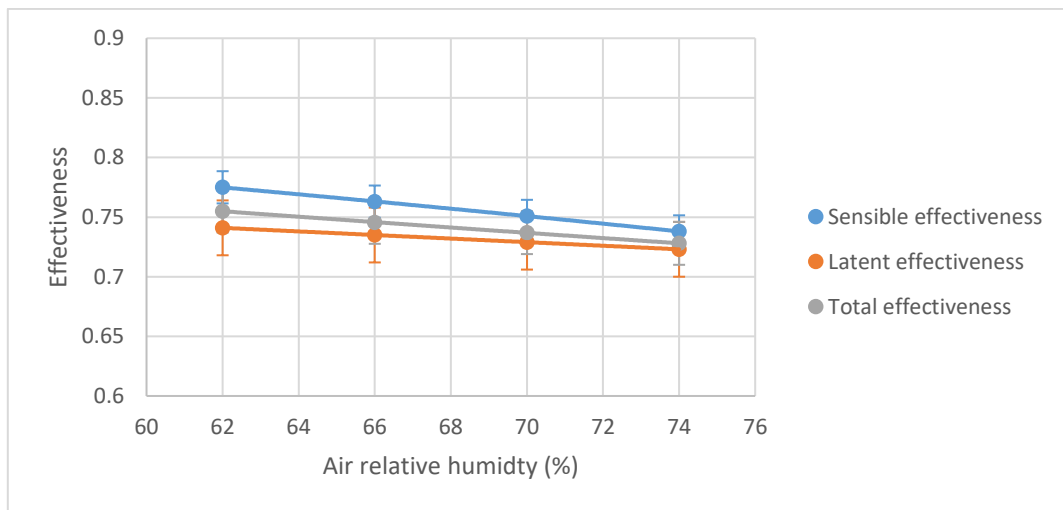
120

121

122

123

From Fig.3 (a), it can be seen that the highest air temperature area is located at the cross section of the air inlet and solution outlet. The air temperature in that area is even higher than the inlet air temperature because the plenty of latent heat is released. As indicated in Fig.3 (b), the highest solution temperature area is located at the bottom-left corner while the lowest temperature field is at the top-right corner. Compared with the previous simulation results shown in Fig.4, the experimental air and solution temperature variation tendencies correspond with the simulated ones. The similar variation tendency can be found in literature [9]. Therefore, the experimental results are convincible and can be used to investigate the LAMEE performance.



124

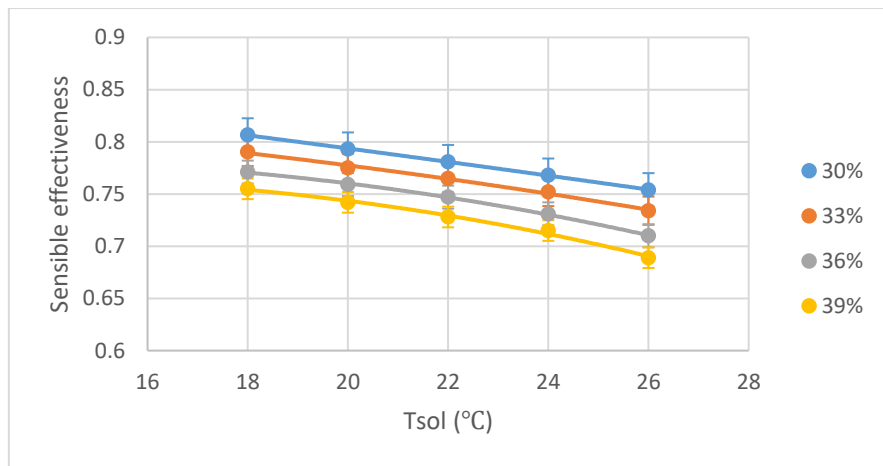
125

Fig. 5: Sensible, latent and total effectiveness variations with air RH.

126 Fig.5 presents the air relative humidity influences on the sensible, latent and total effectiveness
 127 of the LAMEE. Generally speaking, the air RH has little negative influence on the LAMEE
 128 performance. For example, the sensible effectiveness decreases from 0.775 to 0.738 when the
 129 air RH increases from 62% to 76%. The main reason for this case is more latent heat released
 130 in the solution side. In the tested range, the latent effectiveness decreases only about 0.018 but
 131 the moisture remove rate increases 27.38%. Therefore the performance index should be
 132 properly adopted in practical application. The total effectiveness also decreases a little with the
 133 air RH about 0.027 in the tested range.

134

135

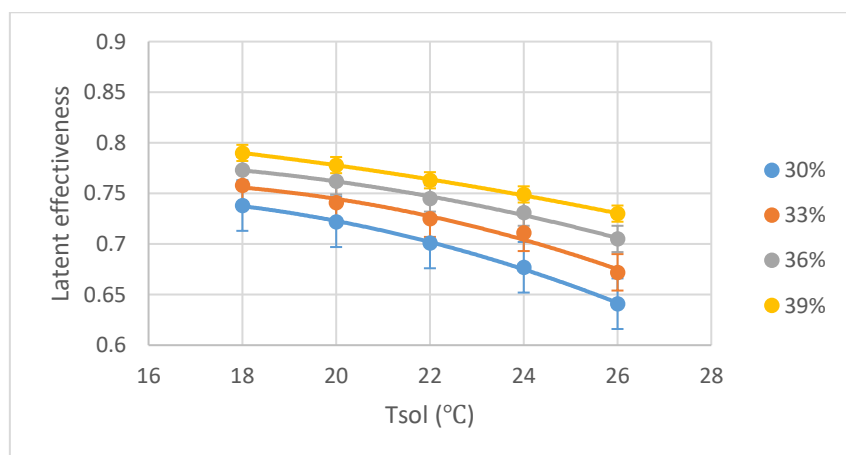


136

137 Fig.6: Sensible effectiveness variations with T_{SOL} under different C_{SOL} .

138

139



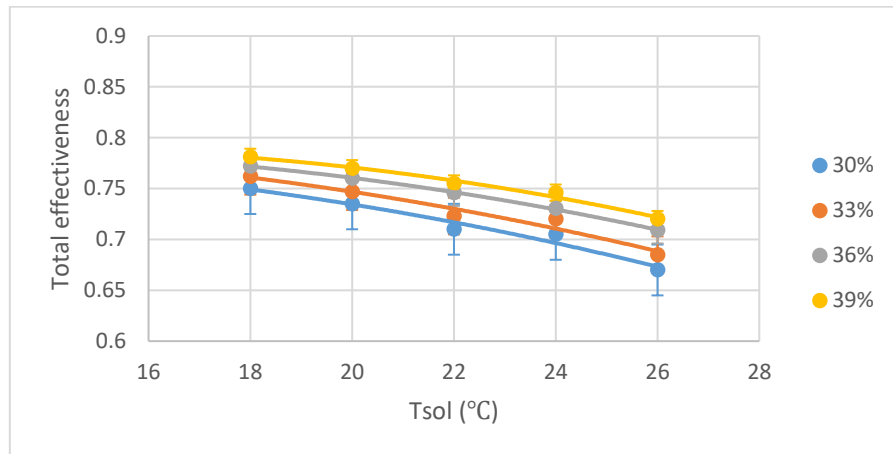
140

141

Fig.7: Latent effectiveness variations with T_{SOL} under different C_{SOL} .

142

143



144

145

Fig.8: Total effectiveness variations with T_{SOL} under different C_{SOL} .

146

147

148

149

150

151

152

153

154

155

Figs.6, 7 and 8 indicate the solution temperature and concentration influences on the effectiveness. It is obvious that the solution temperature has negative influence on the sensible, latent and total effectiveness. Increasing the solution temperature decreases the vapour pressure difference between the air and desiccant solution sides, then reduces the dehumidification performance. Enhancing the solution temperature reduces both the denominator and numerator in Eq. (1) at the same time but with larger numerator reduction. The influence of the liquid desiccant solution temperature on LAMEE performance is more obvious than the air RH's. For example, at $C_{SOL}=33\%$, the total effectiveness reduces from 0.762 to 0.685 when the solution temperature changes from 18°C to 26 °C; while at $C_{SOL}=39\%$, the corresponding total effectiveness decreases from 0.781 to 0.720.

156

157

158

159

160

161

162

As for the solution concentration effect, increasing the solution concentration decreases the sensible effectiveness due to more moisture absorbed. In opposite, the high concentration solution makes contribution to the latent and total effectiveness. However, the influence on the total effectiveness is insignificant. For instance, the total effectiveness decreases from 0.770 to 0.735 when the solution concentration changes from 39% to 30% at the inlet solution temperature of 20 °C. Therefore for the practical application, this should be considered because only 5 percent or less effectiveness improvement is achieved in the experimental test.

163

6. Conclusion

164 In this paper, the temperature field of a cross flow LAMEE is investigated experimentally.
165 Some conclusions can be drawn as follows:

166

- 167 • The experimental temperature fields have the correct variation tendency and can be
168 used to optimise the LAMEE performance.
- 169 • Air relative humidity has little effect on the LAMEE performance. In the tested range,
170 the sensible, latent and total effectiveness only decrease 0.037, 0.018 and 0.027
171 respectively.
- 172 • Desiccant solution temperature has obviously negative influences on the sensible, latent
173 and total effectiveness. At $C_{SOL}=33\%$, the total effectiveness reduces from 0.762 to
174 0.685 when the solution temperature changes from 18 °C to 26 °C; at $C_{SOL}=39\%$, the
175 corresponding total effectiveness decreases from 0.781 to 0.720.
- 176 • The solution concentration has the negative effect on the sensible effectiveness while it
177 has the positive influences on the latent and total effectiveness. However, only less than
178 5% effectiveness improvement is achieved in the experimental test. Therefore, its
179 limited effect should be considered in practical application.

180

181 **Conflict of interest**

182 The authors declared that there is no conflict of interest.

183 **References**

- 184 [1] A.M Omer. Energy, environment and sustainable development. *Renewable and Sustainable*
185 *Energy Reviews* 2008; 12:2265–300.
- 186 [2] X.D Cao, X.L Dai, J.J Liu. Building energy-consumption status worldwide and the state-
187 of-the-art technologies for zero-energy buildings during the past decade. *Energy and*
188 *Buildings* 2016; 128: 198–213.
- 189 [3] K.Daou, R.Z Wang, Z.Z. Xia. Desiccant cooling air conditioning: a review. *Renewable and*
190 *Sustainable Energy Reviews* 2006; 10: 55-77.
- 191 [4] A.H Abdel-Salam, G.M Ge, G.J Simonson. Performance analysis of a membrane liquid
192 desiccant air-conditioning system. *Energy and Buildings* 2013; 62:559–569.
- 193 [5] Y.M Luo, HX Yang, L Lu, RH Qi. A review of the mathematical models for predicting the
194 heat and mass transfer process in the liquid desiccant dehumidifier. *Renewable and*
195 *Sustainable Energy Reviews* 2014; 31:587-599.

- 196 [6] Y.M Luo, HX Yang, Y Chen, YH Wang. Application of CFD Model in Analyzing the
197 Performance of a Liquid Desiccant Dehumidifier. *Energy Procedia* 2016; 88:491-497.
- 198 [7] X.H Liu, Y Jiang, K.Y Qu. Heat and mass transfer model of cross flow liquid desiccant
199 air dehumidifier/regenerator. *Energy Conversion and Management* 2007; 48:546-554.
- 200 [8] S.A Nada. Air cooling-dehumidification/desiccant regeneration processes by a falling
201 liquid desiccant film on finned-tubes for different flow arrangements. *International Journal*
202 *of Thermal Sciences* 2017; 113:10-19.
- 203 [9] R.S Das, S J. Performance characteristics of cross-flow membrane contactors for liquid
204 desiccant systems. *Applied Energy* 2015; 141: 1-11.
- 205 [10] S.M Huang, M.L Yang, X.X Yang. Performance analysis of a quasi-counter flow parallel-
206 plate membrane contactor used for liquid desiccant air dehumidification. *Applied Thermal*
207 *Engineering* 2014; 63:323-332.
- 208 [11] H.Y Bai, J Zhu, Z.W Chen, J.Z Chu. Parametric analysis of a cross-flow membrane-based
209 parallel-plate liquid desiccant dehumidification system: Numerical and experimental data.
210 *Energy and Buildings* 2018; 158:494-508.